Raman Spectroscopy Analysis of Botryococcene Hydrocarbons from the Green Microalga *Botryococcus braunii*[*][S]

Taylor L. Weiss[‡]**, Hye Jin Chun**[§]**, Shigeru Okada**[¶]**, Stanislav Vitha**[||]**, Andreas Holzenburg**[‡||**]**, Jaan Laane**[§]**, and Timothy P. Devarenne**[‡1]

From the [‡]*Department of Biochemistry and Biophysics, Texas A&M University, College Station, Texas 77843-2128, the* [§]*Department of Chemistry, Texas A&M University, College Station, Texas 77843-3255, the* [¶]*Laboratory of Aquatic Natural Products Chemistry, Graduate School of Agricultural and Life Sciences, The University of Tokyo, 1-1-1 Yayoi, Bunkyo-ku, Tokyo 113-8657, Japan, the* [||]*Microscopy and Imaging Center, Texas A&M University, College Station, Texas 77843-2257, and the* [**]*Department of Biology, Texas A&M University, College Station, Texas 77843-2257*

Botryococcus braunii, **B race is a unique green microalga that produces large amounts of liquid hydrocarbons known as botryococcenes that can be used as a fuel for internal combustion engines. The simplest botryococcene (C_{30}) is metabolized by methylation to give intermediates of C_{31}, C_{32}, C_{33}, and C_{34}, with C_{34} being the predominant botryococcene in some strains. In the present work we have used Raman spectroscopy to characterize the structure of botryococcenes in an attempt to identify and localize botryococcenes within *B. braunii* cells. The spectral region from $1600–1700$ cm^{-1} showed ν(C=C) stretching bands specific for botryococcenes. Distinct botryococcene Raman bands at 1640 and 1647 cm^{-1} were assigned to the stretching of the C=C bond in the botryococcene branch and the exomethylene C=C bonds produced by the methylations, respectively. A Raman band at 1670 cm^{-1} was assigned to the backbone C=C bond stretching. Density function theory calculations were used to determine the Raman spectra of all botryococcenes to compare computed theoretical values with those observed. The analysis showed that the ν(C=C) stretching bands at 1647 and 1670 cm^{-1} are actually composed of several closely spaced bands arising from the six individual C=C bonds in the molecule. We also used confocal Raman microspectroscopy to map the presence and location of methylated botryococcenes within a colony of *B. braunii* cells based on the methylation-specific 1647 cm^{-1} botryococcene Raman shift.**

In recent years, interest in the use of green algae as a source of biofuels has increased due to the need to reduce greenhouse gas emissions and because of depletion of world petroleum reserves (1). For algae to produce enough oil to meet fuel demands, large scale culturing of algae and monitoring of oil production will be required (2, 3). Current analysis methods for monitoring algal

oil production are complicated, time consuming, and destructive (4). Thus, a simple and nondestructive method for analyzing algal oil composition is required. Raman spectroscopy is such a technique and has been used to detect various molecular compounds in algae, both to detect algae in aqueous samples and differentiate algal strains, as well as analyze cellular triglycerides, the most common oil used to produce biofuels (4–15). Thus, Raman spectroscopy has great potential to be used as an *in vivo* detection method for monitoring algal oil production.

The green colonial microalgae *Botryococcus braunii* is a prodigious producer of liquid hydrocarbon oils, which are mainly (90–95%) stored in the colony extracellular matrix with the remaining found inside the cells (16–20). There are three races of *B. braunii*, which are classified based on the type of hydrocarbons they produce. The A race produces fatty acid-derived alkadienes and alkatrienes (21–24); the L race produces the tetraterpene lycopadiene (25, 26); and the B race, the focus of this study, produces triterpenes known as botryococcenes (19, 22, 27). Hydrocarbons from all three races of *B. braunii* can be converted into fuels suitable for combustion engines and have been found as major constituents of currently used petroleum and coal deposits (18, 28–39). These attributes have made *B. braunii* an attractive source of renewable biofuels, especially the B race because botryococcenes can be converted into high octane gasoline, kerosene, and diesel fuels (18).

Botryococcenes are biosynthesized through the isoprenoid pathway and are similar in structure to another common triterpene, squalene (40, 41). Both botryococcene and squalene are C_{30} compounds produced by the condensation of two molecules of C_{15} farnesyl diphosphate. However, they differ in how the farnesyl molecules are connected; squalene has a connection of carbon 1′ of one farnesyl molecule to carbon 1 of the second farnesyl molecule (1′–1 connection), whereas C_{30} botryococcene has a 1′–3 connection of the two farnesyl molecules (40, 42). This bonding pattern for botryococcenes produces a central branch with C=C bonds at C-11 and C-26 of C_{30} botryococcene that are not found in squalene (Fig. 1*A*). Once produced, C_{30} botryococcene is further metabolized by methylation at carbons 3, 7, 16, and 20 to produce C_{31}, C_{32}, C_{33}, and C_{34} botryococcenes (19, 43, 44), and even further methylated to C_{36} and C_{37} botryococcenes in some B race strains (22, 45). In C_{34}

[S] The on-line version of this article (available at http://www.jbc.org) contains supplemental Figs. S1–S3.
[1] To whom correspondence should be addressed. Tel.: 979-862-6509; Fax: 979-845-9274; E-mail: tpd8@tamu.edu.

botryococcene-producing strains such as the Berkeley (Showa) strain, the majority (>99%) of the C_{34} botryococcenes exist in the extracellular matrix whereas the intracellular oil comprises predominantly the lower carbon number botryococcenes (19, 20). These botryococcenes are excreted to the extracellular matrix as they mature to C_{34} botryococcene (19, 20). The intracellular botryococcenes are presumed to be located in the numerous intracellular oil bodies found within *B. braunii* cells (16–18). However, there has been no evidence reported to indicate that these intracellular oil bodies actually contain botryococcenes or any other classes of lipids such as triglycerides. Moreover, if these oil bodies are actually composed of botryococcenes, there is no information as to what kinds of botryococcene homologs exist in the droplets.

Spectroscopic characterization, other than NMR, of *B. braunii* hydrocarbons is extremely limited (13, 46). A characteristic absorbance spectroscopy peak for botryococcenes has been identified and used to quantitate extracted botryococcenes (46). Raman spectroscopy has been used on the A race of *B. braunii* to determine that the intracellular oils were similar in nature to the extracellular oils and that these oils were composed of long chain unsaturated hydrocarbons (13). Specific characterization by Raman spectroscopy for any hydrocarbon from any race of *B. braunii* has not been reported. There are several C=C bonds in botryococcenes that offer unique Raman spectroscopic parameters. For example, the methylation of C_{30}–C_{33} botryococcenes causes C=C bond migration from the backbone endo positions to exo positions at carbons 2, 6, 17, and 21 to create exomethylene groups (Fig. 1*A*). Additionally, the C-26 branch C=C bond is specific to botryococcenes. In our present work we report characterization of botryococcenes from the B race of *B. braunii* by Raman spectroscopy and density function theory (DFT)[2] calculations. Additionally, an identified Raman signature specific to methylated botryococcenes is used to map *in vivo* the presence of methylated botryococcenes in the extracellular matrix and intracellular oil bodies of live *B. braunii* cells.

EXPERIMENTAL PROCEDURES

Algal Culturing—*B. braunii*, Berkeley (Showa), B race (47) were grown in modified Chu 13 media (48) using 13-W compact fluorescent 65 K lighting at a distance of 7.62 cm, which produced a light intensity of 280 μmol photons $\cdot$ m^{-2} $\cdot$ s^{-1}. Lighting was on a cycle of 12-h light:12-h dark at 22.5 °C. The cultures were continuously aerated with filter-sterilized, enriched air containing 2.5% CO_2. Fifty ml of culture was used to inoculate 750 ml of subsequent subcultures every 4 weeks. The remaining culture volume was harvested by vacuum filtration using 35 μM nylon mesh (Aquatic Ecosystems, Inc., Apopka, FL). The accumulated colonies were rinsed with sterilized dH$_2$O, frozen in liquid nitrogen, and stored at −80 °C.

Purification and Structural Determination of B. braunii Botryococcenes—Botryococcenes were purified from freeze-dried *B. braunii* samples as described previously (49, 50). In brief, 10 g of freeze-dried *B. braunii* cells was extracted in *n*-hexane to remove extracellular hydrocarbons followed by a chloroform:methanol (2:1) extraction to remove intracellular

hydrocarbons. Both extracts were evaporated to dryness, resuspended in *n*-hexane, combined, applied to an *n*-hexane gravity-fed silica column, and a total hydrocarbon fraction was collected as the eluate prior to the pigment front. The total hydrocarbon fraction was evaporated to dryness, resuspended in 0.5 volume of acetone, and separated by HPLC using a 20 × 250-mm Cosomil 5C$_{18}$-AR-II column with 100% MeOH mobile phase at a flow rate of 9 ml/min, detection at 210 nm. Botryococcenes eluted as follows: C_{30} botryococcene (~27 min), C_{32} and C_{33} in one peak (~30 min). To separate impurities from C_{30} botryococcene and to separate C_{32} and C_{33} botryococcenes, samples were applied sequentially to a 20 × 250-mm Develosil 60 silica, 3-μm HPLC column with 100% *n*-hexane mobile phase at a flow rate of 8 ml/min, detection at 210 nm. Botryococcenes eluted as follows: C_{30} botryococcene (~32 min), C_{32} (~27 min), and C_{33} (~25 min). Purity of the isolated botryococcenes was analyzed with a Shimadzu GC-2014 with a 60-m DB-1 column (J & W Science), 0.25-mm inner diameter, 0.25-μm film, helium carrier gas, 250-kPa head pressure, 250 °C injection temperature, FID detector at 260 °C, and a temperature program of 50 °C for 1 min, raised to 220 °C at 10 °C/min, raised to 260 °C at 2 °C/min, hold at 260 °C for 40 min. Botryococcenes retention times as follows: C_{30} botryococcene (~42 min), C_{32} (~46 min), and C_{33} (~48 min). A C_{34} botryococcene was obtained from a previous analysis (50). The molecular mass of all purified botryococcenes was confirmed by fast atom bombardment-mass spectroscopy using *m*-nitrobenzyl alcohol as a matrix on a JEOL SX 102 mass spectrometer, and their plane structures were confirmed by measuring ^{1}H and ^{13}C NMR spectra in CDCl$_3$ using a JEOL alpha 600 NMR spectrometer at 600 MHz and 150 MHz, respectively. The NMR data were compared with those for known botryococcenes (41, 49).

Raman Spectroscopy—Raman spectra of squalene (Sigma), total hydrocarbon extract, and purified botryococcenes (all in *n*-hexane in a cuvette) were obtained at Horiba Scientific (Edison, NJ) using a Horiba LabRam HR 800 confocal Raman microscope. The Raman spectrometer was coupled with an Olympus BXFM microscope and a liquid nitrogen-cooled CCD detector. The excitation source was a Melles-Griot laser operating at 532 nm with a 50-mW output. A singlet lens with a focal length of 40 mm was used.

Raman spectra of squalene and total hydrocarbon extract contained in vials without solvent were also recorded with a Jobin Yvon U-1000 double monochromator equipped with a liquid nitrogen-cooled CCD detector. A Coherent Verdi-V10 laser operating at 532 nm was utilized as the excitation source. A laser power of 2 W was typically used.

In vivo mapping by confocal Raman spectroscopy was performed at the Texas A&M Materials Characterization Facility using a Horiba Jobin Yvon LabRam IR system with an Olympus BX 41 microscope, a computer-controlled motorized XYZ microscope stage, and a liquid nitrogen-cooled CCD detector. Excitation was achieved with a laser wave length of 785 nm at an output power of 20 mW. The spectral maps were recorded with a spectral resolution of 0.16 cm^{-1} and pixel size of 275 nm with an UPLSAPO 100×/1.4 oil immersion objective. Cell photobleaching was performed using a 785-nm laser at a power output of 500 mW for at least 20 min. Exact treatment times varied

---

[2] The abbreviation used is: DFT, density function theory.

as colony cell density varied across the *z* axis. Photobleaching was considered complete once the high, consistent Raman intensities across 200–3600 cm^{-1} sufficiently decreased to allow detection of individual Raman peaks and remained static for at least 2 min.

All Raman spectra were collected in 60-cm^{-1} segments with accumulation times of 1000 s for each segment. Spectra were analyzed for peak wavenumbers using the LabSpec program version 5.58.25.

DFT Calculations—DFT computations used the GAUSSIAN 03 package (51) to obtain the calculated vibrational frequencies and produce the computed Raman spectra. The B3LYP/cc-pvtz basis set was utilized. A scaling factor of 0.969 was applied for all frequencies. This value was selected to match the observed and calculated ν(C=C) stretching frequencies for squalene. The computed spectra were produced using the GaussView 4.1.2 program.

Microscopy and Nile Red Staining—Microscopy imaging of *B. braunii* colonies was performed at the Texas A&M University Microscopy and Imaging Center. For visualization of botryococcenes using Nile red (Sigma), 1 ml of *B. braunii* colonies in medium at stationary phase density were treated with 2.5 μl of a stock solution of Nile red dissolved in acetone (0.15 mg/ml) so that the final concentrations of Nile red and acetone were 0.375 μg/ml and 0.25%, respectively. Samples were kept in the dark and incubated at room temperature for 15 min. Fluorescence microscopy visualization was performed with a Zeiss Axiophot microscope equipped with a GFP filter set (excitation, 450–490 nm; emission, 500–550 nm), Plan Neofluar 100×/1.3 oil immersion objective, and a Coolsnap CF monochrome CCD camera (Photometrics, Tucson, AZ) controlled by MetaView version 5.2 software (Molecular Devices, Downingtown, PA). For transmitted light imaging, differential interference contrast optics and a Nikon DXM1200C (Nikon Instruments, Melville, NY) color CCD camera were used on the same microscope.

RESULTS AND DISCUSSION

B. braunii System Description—Most of the botryococcene oils in *B. braunii*, B race, localize to the colony extracellular matrix and can be released with pressure (Fig. 1*B*). It is well known that *B. braunii* cells also have many intracellular oil bodies (16–18) (Fig. 1*B*). Both these intracellular oil bodies and extracellular oil can be visualized using the fluorescent neutral lipid-binding stain Nile red, which has been used to accurately estimate *B. braunii* oil content in high-throughput screens (52–54). Therefore, we used fluorescence microscopy and Nile red to show the dramatic accumulation of lipids in the extracellular matrix and in intracellular oil bodies (Fig. 1*C*). Lipids detected by Nile red fluorescence (white to gray signal) show that each cell of the colony contains many individual oil bodies (Fig. 1*C*). As mentioned above, the lipid composition of these intracellular oil bodies is not known; i.e. do they contain botryococcenes? If so, do all oil bodies consist of one molecular species of botryococcene, or are they a mixture of all botryococcenes? Because Nile red is a bulk lipid-binding molecule it does not differentiate among the different botryococcenes species and cannot be used to address these questions. Thus, the ultimate
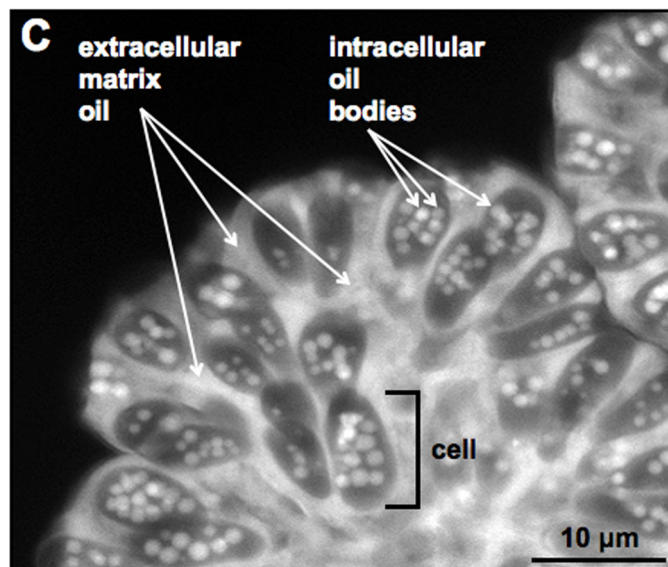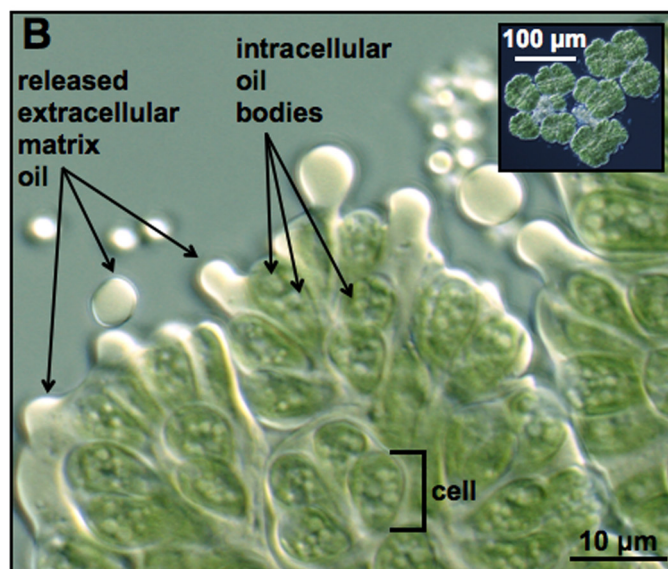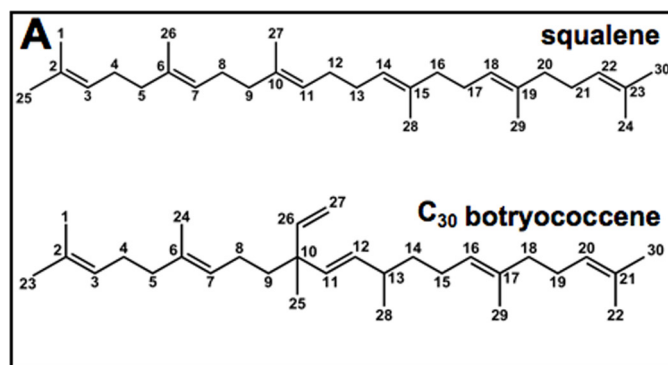
FIGURE 1. **Microscopy and Nile red fluorescent imaging of *B. braunii* cells.** *A*, structure of squalene and C$_{30}$ botryococcene. *B*, transmitted light microscope image of a partial *B. braunii* colony showing pressure-released extracellular oil and intracellular oil bodies. A *B. braunii* colony was subjected to pressure by gently pressing on the microscope slide coverslip to expel extracellular oil. *Inset* shows full *B. braunii* colony for perspective. *C*, colony of *B. braunii* treated with Nile red and viewed by fluorescent microscopy to visualize the Nile red-stained extracellular matrix oil and intracellular oil bodies.
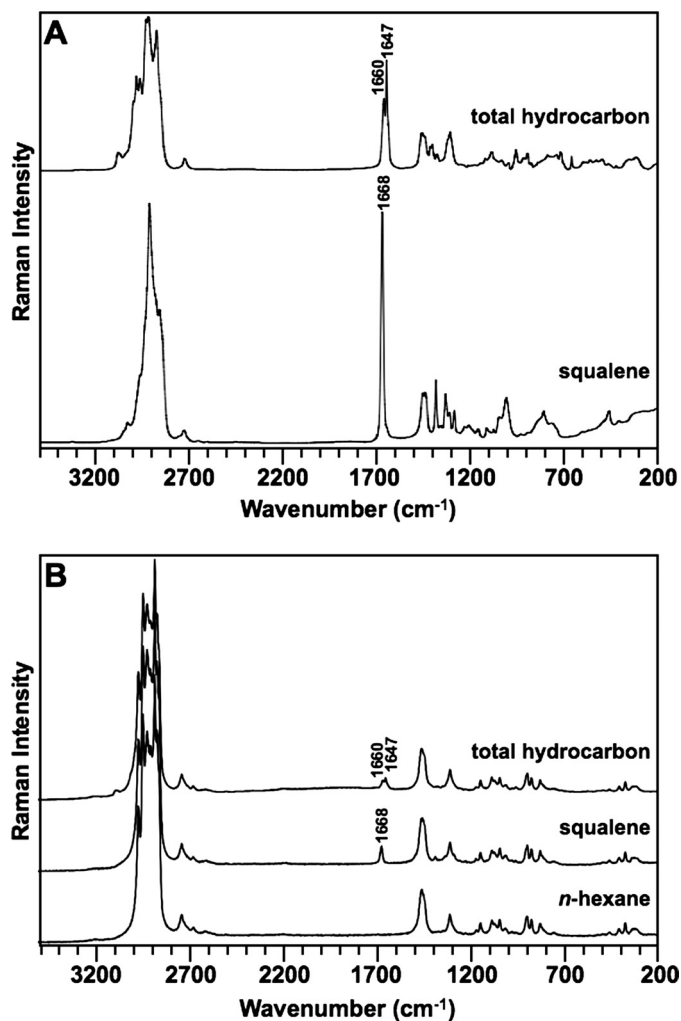
FIGURE 2. **Raman spectra of squalene and total *B. braunii* hydrocarbons.** *A*, total hydrocarbon extract from *B. braunii* and a pure, commercially acquired squalene sample were analyzed by Raman spectroscopy without solvent. *B*, *B. braunii* total hydrocarbon extract and squalene samples from *A* were solubilized in *n*-hexane and analyzed by Raman spectroscopy. Analysis was performed on *n*-hexane alone to determine background Raman spectra.

goal of our research is to use Raman microspectroscopy to detect specific botryococcenes within both the extracellular matrix and intracellular oil drops to begin to address the questions about oil body botryococcene composition. The use of a confocal Raman microscope for the investigation of intracellular oil drops has the potential to eliminate the out-of-focus signal and suppress the inherently high autofluorescence background from the large chloroplast sheet enveloping the cell.

Experimental Raman Spectra for Botryococcenes—To identify spectral regions that contain specificity for botryococcenes, Raman spectroscopy was applied to squalene and a total hydrocarbon extract from *B. braunii*, B race. Because a total hydrocarbon extract from some strains of the B race of *B. braunii*, for example the Berkeley strain, is predominantly C_{34} botryococcene (41, 49, 50) and GC analysis of our total hydrocarbon extract shows C_{34} botryococcene as the primary constituent (see supplemental Fig. S1), comparison of the two spectra should indicate regions unique to botryococcenes. Analysis of the two spectra indicates similarity across the spectra (Fig. 2*A*). However, we chose to focus on the 1600–1700 cm^{-1} region for

ν(C=C) stretching vibration because the main structural differences between squalene and botryococcenes are in the C=C bond positions. Within this spectral region, squalene generated a single band at 1668 cm^{-1}, and the total hydrocarbon fraction generated two bands at 1647 and 1660 cm^{-1} (Fig. 2*A*). Because the subsequent analysis of purified botryococcenes was performed in *n*-hexane (see below), the Raman spectra of squalene and total hydrocarbons dissolved in *n*-hexane were analyzed to ensure that the difference in the ν(C=C) stretching region could still be detected in the presence of *n*-hexane. As shown in Fig. 2*B*, the 1600–1700 cm^{-1} ν(C=C) stretching region of the spectra of squalene and total hydrocarbons in *n*-hexane shows the same bands seen without *n*-hexane. However, the absolute intensity was reduced (compare Fig. 2, *A* and *B*). The *n*-hexane sample alone did not show these bands (Fig. 2*B*).

Next, Raman spectroscopy was applied to individual botryococcenes in *n*-hexane and analyzed in the ν(C=C) stretching region to identify bands specific to the botryococcene structure. Pure C_{30}, C_{32}, C_{33}, and C_{34} botryococcenes were obtained by HPLC, purity was confirmed by GC, molecular weights were confirmed by fast atom bombardment-mass spectroscopy, and structures were confirmed by NMR as described previously (41, 49, 50). We were unable to purify sufficient quantities of C_{31} botryococcene to analyze by Raman spectroscopy at this time and obtained a minimal amount of C_{30} botryococcene (3 mg) to obtain a workable spectrum. Analysis of all bands identified in the 1600–1700 cm^{-1} ν(C=C) stretching region of the spectra reveals that several of the bands can be assigned to specific bonds in botryococcenes. The band at 1647 cm^{-1} is seen in all botryococcenes except for C_{30} botryococcene (Fig. 3*A*). Because C_{30} botryococcene lacks methylation (Fig. 3*B*), this suggests that the 1647 cm^{-1} band originates from the exomethylene groups generated by the methylation events. The band at 1670 cm^{-1} is seen in all botryococcenes except C_{34} botryococcene (Fig. 3*A*), suggesting that it is due to the backbone C=C bonds because C_{34} botryococcene lacks these bonds with the exception of the C=C bond at C-11 (Fig. 3*B*). Moreover, squalene, which possesses only backbone C=C bonds, has its maximum Raman intensity at 1668 cm^{-1}. The bands at 1639 and 1660 cm^{-1} are more difficult to assign but appear to be specific to botryococcenes compared with squalene (Fig. 3*A*). These bands may be assigned to the branch C=C bond at C-26 and the backbone C=C bond at C-11 that are found in all botryococcenes (Fig. 3*B*). This is supported by the spectrum for C_{34} botryococcene (Fig. 3*A*), which has three major bands: 1647 cm^{-1} attributed to the exomethylene groups and 1639 and 1660 cm^{-1}, which should be attributable to the C-26 and C-11 C=C bonds because they are the only other C=C bonds in C_{34} botryococcene (Fig. 3*B*). However, with these data it is difficult to assign these bands specifically to the C-26 or C-11 C=C bonds. A band at 1634 cm^{-1} is also seen in C_{32} botryococcene which cannot be assigned at this time.

These Raman spectra indicate that the Raman bands of 1639, 1647, 1660, and 1670 cm^{-1} are specific for botryococcenes. Thus, these bands could be used as diagnostic signatures for the presence of botryococcenes. The 1647 cm^{-1} band is specifically due to botryococcene methylation and may offer the best signature for Raman spectroscopy identification of botryococc-
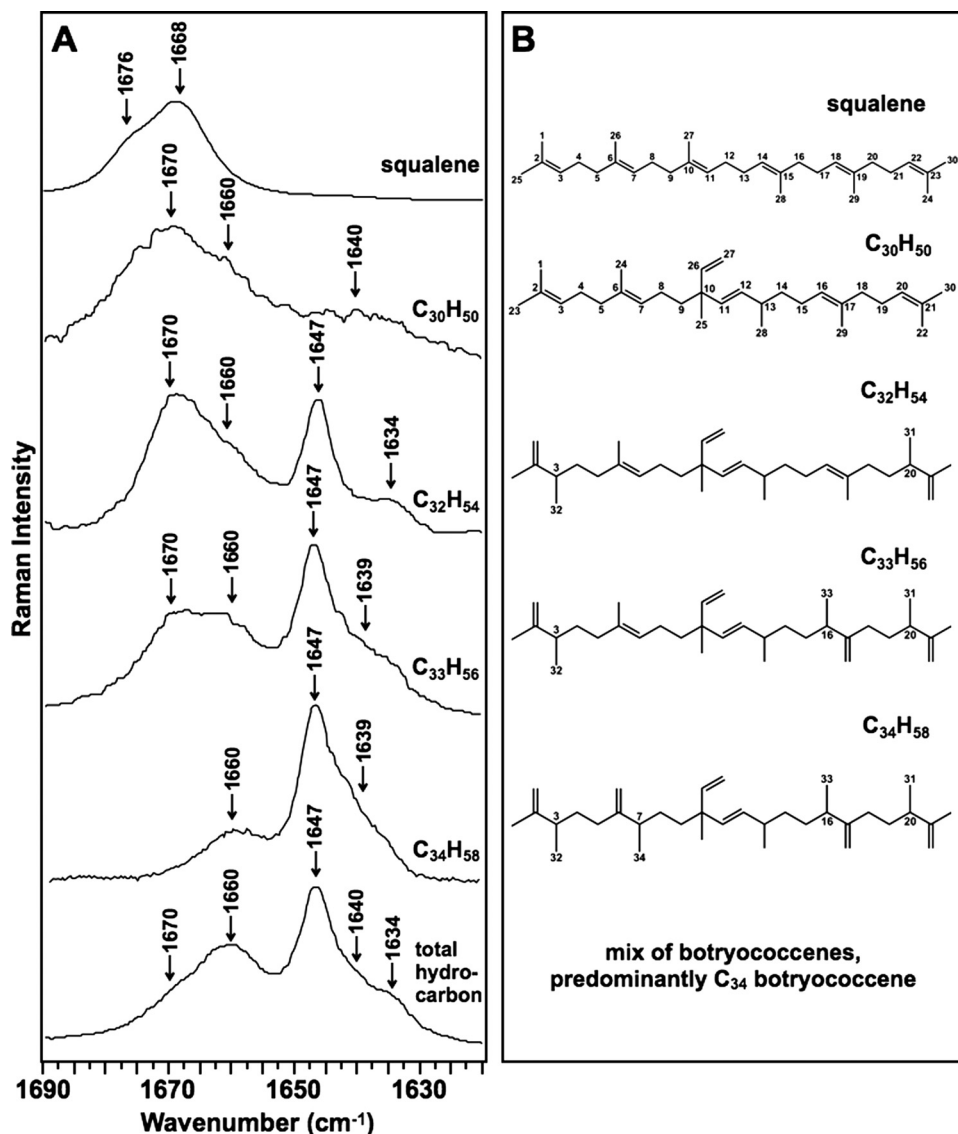
FIGURE 3. **Raman spectra for the ν(C=C) stretching region of botryococcenes.** *A*, indicated botryococcenes were purified from *B. braunii* by HPLC, dissolved in *n*-hexane, analyzed by Raman spectroscopy within the ν(C=C) stretching region, and compared with that for the total hydrocarbon extract and pure squalene. *B*, structures of squalene and individual botryococcenes analyzed in *A*.

tra from the calculations indicate that the major differences among all the botryococcenes analyzed are in the ν(C=C) stretching region as seen in the experimental spectra (Fig. 4*B*). Analysis of the 1600–1700 cm^{-1} region for ν(C=C) stretching shows strong similarities to our experimental spectra (Fig. 5). Fig. 5 shows the computed spectra for this region, and Table 1 lists the calculated wavenumber values and compares them with those observed experimentally. It should be noted that each molecule has six independent ν(C=C) stretching frequencies, but these may overlap to produce only two or three Raman bands depending on the type (backbone, exomethylene, or branch) of C=C bond present. Fig. 6 shows the individual stretching frequency calculated for each specific C=C bond for each of the molecules. Remarkably, the stretching vibration of each individual C=C bond is shown by the calculations to be almost totally independent and uncoupled to any of the other ν(C=C) stretching motions or to any other vibration. What is clearly evident from Figs. 5 and 6 and Table 1 is that the three types of ν(C=C) stretching vibrations fall into distinct spectral regions. The backbone ν(C=C) stretching wavenumbers are calculated to be between 1663 and 1679 cm^{-1} for all the molecules and are observed in the 1660–1670 cm^{-1} region. The exomethylene stretches are calculated to be between 1646 and 1655 cm^{-1} and are all observed at 1647 cm^{-1}. The branch C=C stretches are computed to be in the 1642–1649 cm^{-1} range and are experimentally observed at 1639–1640 cm^{-1}.

Because the calculated Raman spectra were determined for fixed bonds of a linear botryococcene structure, we analyzed how different conformations of the botryococcene structure would affect the Raman spectra. The spectra for three different conformers of C_{30} botryococcene were calculated based on rotation of the bond at C-18, C-15, or C-5 (supplemental Fig. S2*A*). The full Raman spectra of these conformers appear to be very similar to that of the experimental and calculated spectra for linear botryococcenes (supplemental Fig. S2*A*). However, analysis of the 1600–1700 cm^{-1} ν(C=C) stretching region shows that the spectra of the C_{30} botryococcene conformers have three bands similar to the linear C_{30} botryococcene, but the intensity of the bands varies depending on the conformation (supplemental Fig. S2*B*). This would indicate that different

cenes. This is supported by the Raman spectrum of the total hydrocarbon fraction, which shows the four main botryococcene-specific bands of 1639, 1647, 1660, and 1670 cm^{-1} (Fig. 3*A*). Additionally, the band of 1634 cm^{-1} was detected in the total hydrocarbon fraction that was seen for C_{32} botryococcene and cannot be assigned at this time (Fig. 3*A*). It should be noted that the increasing methylation of botryococcenes is correlated with a shift of bands in the Raman spectra from the 1670 cm^{-1} region toward the 1647 cm^{-1} region (Fig. 3*A*).

Computational Analysis—Because we could not obtain sufficient quantities of C_{31} botryococcene for Raman spectroscopy and could not specifically assign the 1639 and 1660 cm^{-1} bands (Fig. 3*A*), DFT calculations were used to address these problems as well as support our experimental spectra interpretation. There are two isomers of C_{31} botryococcene (Fig. 4*A*) that have been identified in *B. braunii* by methylation of C_{30} botryococcene at C-3 or C-20 (49, 50, 55) (Fig. 4*A*). The full Raman spec-
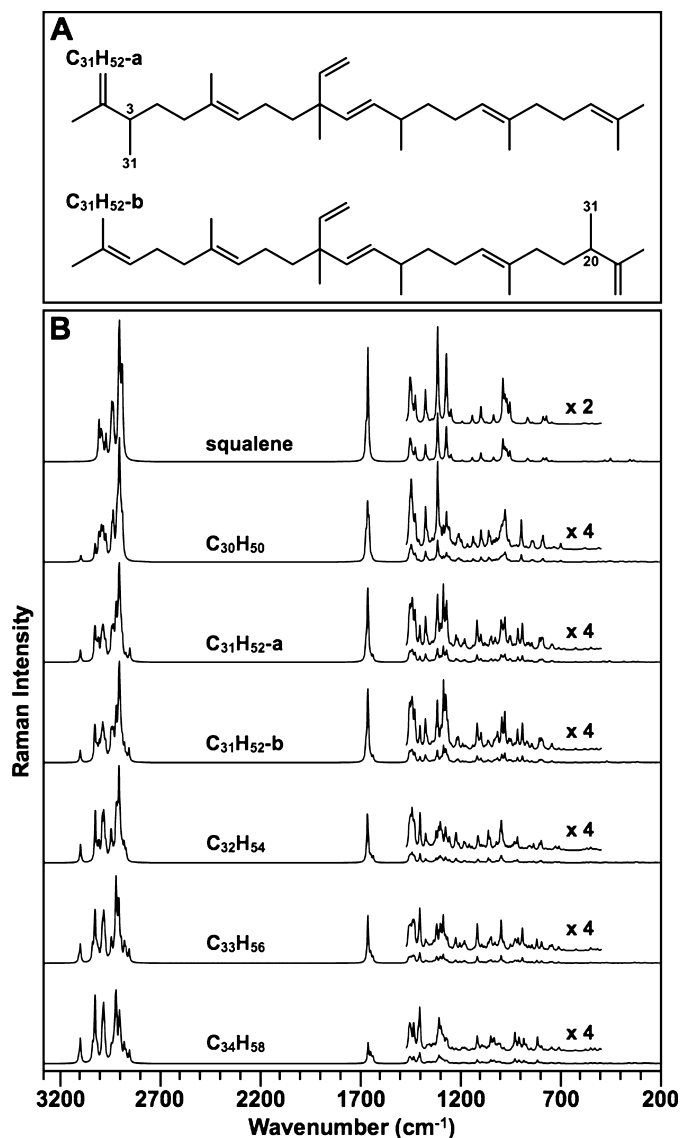
FIGURE 4. **DFT-calculated Raman spectra for botryococcenes.** *A*, structure of the two forms of C_{31} botryococcene identified in *B. braunii*. *B*, DFT-calculated Raman spectra for squalene and the indicated botryococcenes. DFT calculations were performed using the GAUSSIAN 03 package, and the computed spectra were assembled using the GaussView 4.1.2 program.

FIGURE 5. **DFT-calculated Raman spectra for squalene and all botryococcenes in the ν(C=C) stretching region.** All calculations and spectra were generated as in Fig. 4.

conformers of C_{30} and other botryococcenes may not be easily identifiable by Raman spectroscopy in a cell sample with a complex mixture of botryococcenes.

It should be noted that each of these molecules has a large number of vibrations ($3N-6$ where N = number of atoms), and all of these are Raman-active. Thus, for example, $C_{34}H_{58}$ has 270 vibrations. These include 58 C–H stretching modes between 2800 and 3200 cm^{-1} and 33 skeletal stretching vibrations, including the ν(C=C) stretching modes. The remainder are various types of angle bending, twisting, wagging, rocking, etc. motions, and all are below 1500 cm^{-1}. In our present work we focus on the ν(C=C) stretching vibrations (1600–1700 cm^{-1}) because these are well separated from all other modes and provide the means for discriminating between the different botryococcenes and their three types of C=C double bonds (backbone, exomethylene, and branch).
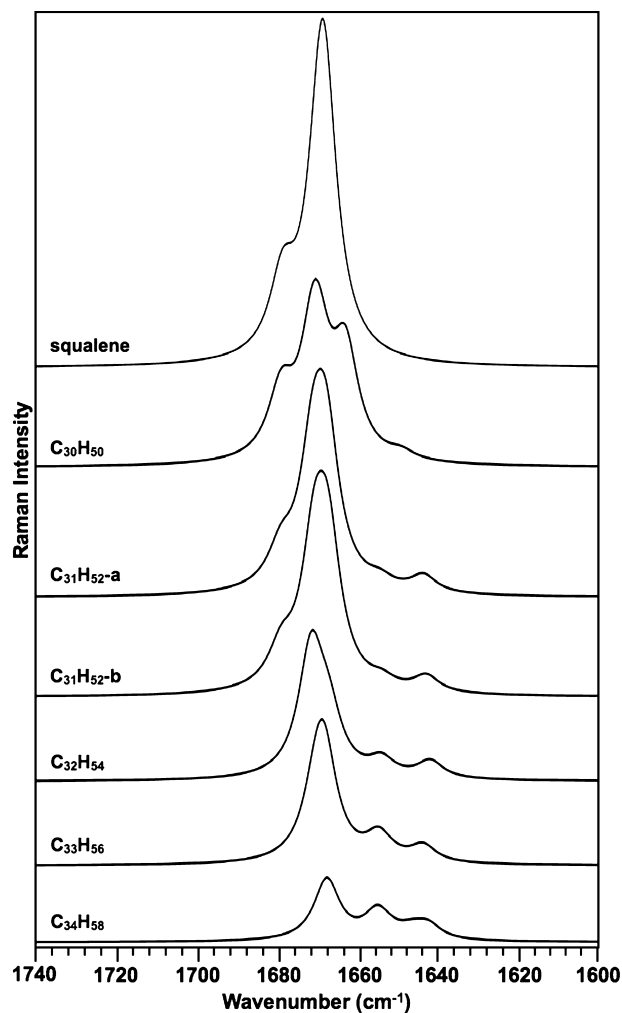
TABLE 1

Comparison of observed and calculated Raman bands for botryococcenes

Molecule	C=C type	Bond number (as shown in Fig. 6)	Frequency range	
			Observed	Calculated
			cm^{-1}	*cm*$^{-1}$
$C_{30}H_{50}$	Backbone	1, 2, 4, 5, 6	1670	1663–1679
	Exomethylene	NP[a]	NP	NP
	Branch	3	1640	1649
$C_{31}H_{52}$-a	Backbone	2, 4, 5, 6	ND[b]	1668–1679
	Exomethylene	1	ND	1654
	Branch	3	ND	1643
$C_{31}H_{52}$-b	Backbone	1, 2, 4, 5	ND	1667–1679
	Exomethylene	6	ND	1654
	Branch	3	ND	1643
$C_{32}H_{54}$	Backbone	2, 4, 5	1670	1667–1671
	Exomethylene	1, 6	1647	1654
	Branch	3	1639	1642
$C_{33}H_{56}$	Backbone	2, 4	1670	1668–1670
	Exomethylene	1, 5, 6	1647	1652–1655
	Branch	3	1639	1644
$C_{34}H_{58}$	Backbone	4	1660	1668
	Exomethylene	1, 2, 5, 6	1647	1646–1655
	Branch	3	1639	1642

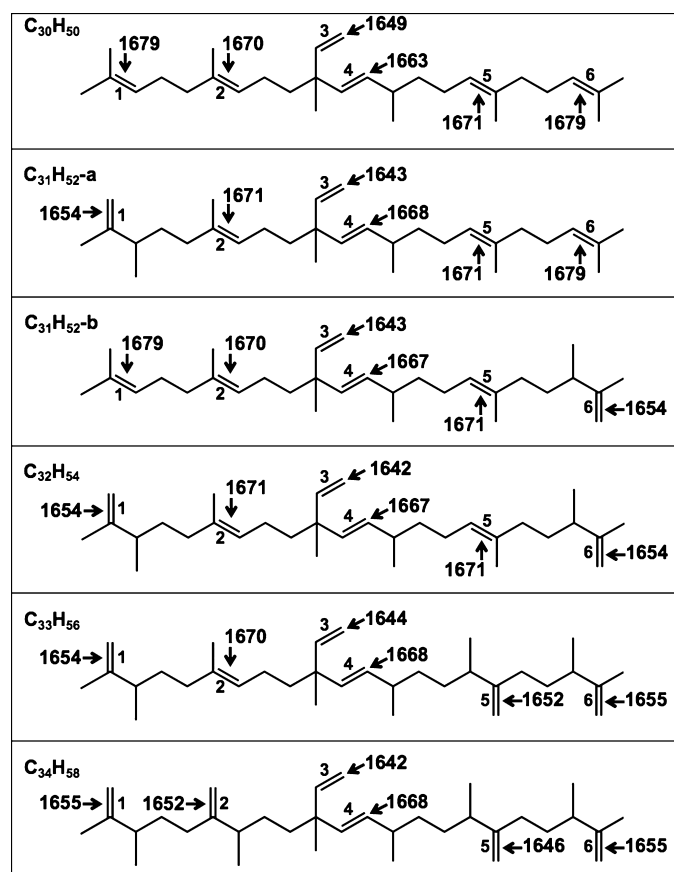[a] Not present in this structure.
[b] Not determined.

FIGURE 6. **Calculated Raman wavenumbers for each C=C bond of individual botryococcenes.** *Numbers 1–6 indicate bond number for reference in Table 1.*
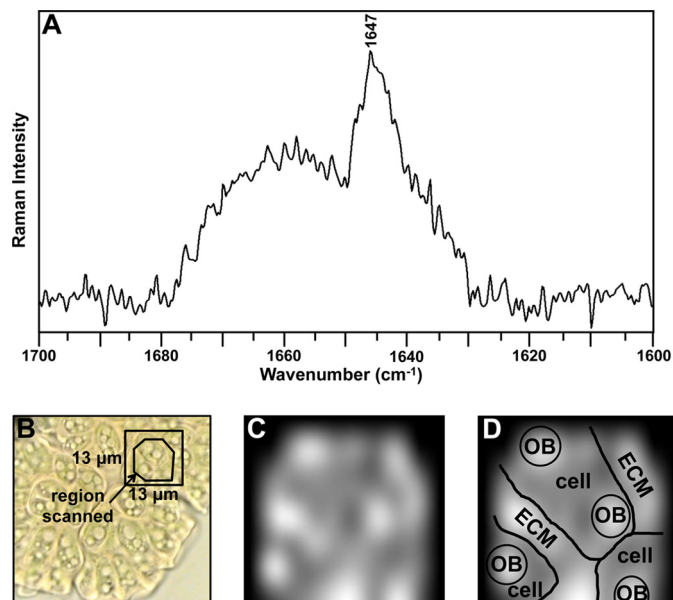

FIGURE 7. **Mapping of methylated botryococcenes in a *B. braunii* colony.** *A, in vivo* Raman spectrum of a *B. braunii* colony. The laser of the confocal Raman microscope was focused on a 13×13-μm region of a colony of *B. braunii*, as shown in *B*, and the Raman spectrum of the region recorded. *B*, light microscope image of the *B. braunii* colony before photobleaching for Raman spectroscopy. *Boxed region* indicates region used for analysis in *A*. *C*, mapping of the 1647 cm^{-1}-specific botryococcene Raman band in the *B. braunii* colony. *D*, graphical representation of colony structure in *C*. *OB*, oil body; *ECM*, extracellular matrix.

In Vivo Raman Spectroscopy Mapping of Botryococcenes—The Raman spectroscopy analysis presented here indicates that specific Raman bands can be used as markers for the presence of botryococcenes in live *B. braunii* cells and/or colonies. This is especially true for the 1647 cm^{-1} band that is specific for indicating the presence of methylated botryococcenes (Fig. 3*A*). Thus, Raman microspectroscopy was applied to a colony of *B. braunii* to map the presence of botryococcenes in the extracellular matrix and intracellular oil bodies. A roughly circular region within a 13×13-μm area of a *B. braunii* colony was scanned as shown in Fig. 7*B*. Raman spectroscopy required photobleaching the cells because chlorophyll autofluorescence caused high background that interfered with detection of botryococcene-specific Raman bands (supplemental Fig. S3). Spectroscopy was implemented after photobleaching, and the Raman spectrum in the 1700–1600 cm^{-1} region is shown in Fig. 7*A*. Detection of the botryococcene methylation-specific 1647 cm^{-1} band was evident and was the most prominent band in the spectrum (Fig. 7*A*). The high level of background within this spectrum prevented us from defining other botryococcene-specific bands.

Next, we mapped the detection of the botryococcene methylation-specific 1647 cm^{-1} band at 54 points yielding a spectral map of the scanned region of the *B. braunii* colony. The presence of the 1647 cm^{-1} band was assigned a white color with diminishing detection levels of the 1647 cm^{-1} band scaled to

gray. Because our cells were photobleached prior to Raman analysis, the cells and extracellular matrix could not be distinguished by a microscopy image. Thus, Fig. 7*D* shows a graphical representation of the colony and cell structure. The results show, as expected and reported (19, 43, 44), that the extracellular matrix has high amounts of methylated botryococcenes (Fig. 7, *C* and *D*), likely C$_{34}$ botryococcene because it is mostly found in the extracellular matrix (16–20). The intracellular oil bodies also contained methylated botryococcenes as determined by detection of the 1647 cm^{-1} band (Fig. 7, *C* and *D*). Unfortunately, we were not able to determine the specific botryococcene makeup of the individual oil bodies beyond the presence of methylated botryococcenes because we were not able to assign and map additional Raman bands due to the high background in our analysis and sample degradation from prolonged interrogation (Fig. 7*A*).

B. braunii also produces squalene-based hydrocarbons that contain exomethylene groups similar to that found in botryococcenes. Tetramethylsqualene is produced by methylation at C-3, -7, -18, and -22 of squalene, which produces exomethylene groups at C-1, -26, and -29, and -24 (49, 56, 57). Tetramethylsqualene can also be combined with long chain polyaldehydes and carotenoids to produce polyacetals and botryoxanthins, respectively (58–60). Because of the exomethylene similarities between methylated botryococcenes and tetramethylsqualene, it is possible that our detection of the 1647 cm^{-1} band in the *B. braunii* colony (Fig. 7*A*) is partially attributable to tetramethylsqualene and its derivatives. However, the levels of free tetramethylsqualene and botryoxanthins in *B. braunii* colonies are minute (0.009–0.033% dry weight) (49, 56, 58–60) and thus, unlikely to be detected by our Raman system. However,

one strain of *B. braunii*, race B, contains levels of methylated squalenes up to 4.5% dry weight (57). Levels of tetra-methylsqualene polyacetals are much higher and can comprise up to 10% of algal dry weight (58). This suggests that *in vivo* Raman microspectroscopy detection may be possible and that these compounds may contribute to the detection and mapping of the 1647 cm^{-1} band in Fig. 7. But, it should be noted that tetramethylsqualene polyacetals are found predominantly within the *B. braunii* cell walls and not in oil bodies or the extracellular matrix (58). Exact wavenumber assignment to the C=C bonds in tetramethylsqualene and its derivatives will require isolation of pure compounds and Raman spectroscopy analysis. Given the difficulty in isolating milligram quantities of these compounds, DFT calculations may offer the best approach for estimating wavenumber assignments.

These studies have identified specific Raman spectroscopic characteristics for botryococcenes of *B. braunii*, B race. Additionally, a botryococcene methylation-specific Raman signature can be detected in living *B. braunii* cells, indicating that Raman spectroscopy is a powerful tool that can be applied to advancing studies on botryococcene biosynthesis. A goal for future studies is to refine the Raman microspectroscopy using instrumentation appropriate to very small photosynthetic cells to fine-map the presence of the different botryococcene homologs in a colony of *B. braunii*. Of particular interest will be the location of the different botryococcenes within the cells to determine whether there is a biosynthetic, or composition difference among the many intracellular oil bodies. Additionally, Raman spectroscopy could be applied to analyze botryococcenes levels and quality during the development of a *B. braunii* culture to determine when oil levels are of both maximal quantity and quality for cell harvesting.

REFERENCES

1. Hu, Q., Sommerfeld, M., Jarvis, E., Ghirardi, M., Posewitz, M., Seibert, M., and Darzins, A. (2008) *Plant J.* **54,** 621–639
2. Chisti, Y. (2008) *Trends Biotechnol.* **26,** 126–131
3. Chisti, Y. (2007) *Biotechnol. Adv.* **25,** 294–306
4. Huang, Y. Y., Beal, C. M., Cai, W. W., Ruoff, R. S., and Terentjev, E. M. (2010) *Biotechnol. Bioeng.* **105,** 889–898
5. Wood, B. R., Heraud, P., Stojkovic, S., Morrison, D., Beardall, J., and McNaughton, D. (2005) *Anal. Chem.* **77,** 4955–4961
6. Wagner, W. D., and Waidelich, W. (1986) *Appl. Spectrosc.* **40,** 191–196
7. Wu, Q., Nelson, W. H., Hargraves, P., Zhang, J., Brown, C. W., and Seelenbinder, J. A. (1998) *Anal. Chem.* **70,** 1782–1787
8. Brahma, S. K., Hargraves, P. E., Howard, W. F., and Nelson, W. H. (1983) *Appl. Spectrosc.* **37,** 55–58
9. Chen, M., Zeng, H., Larkum, A. W., and Cai, Z. L. (2004) *Spectrochim. Acta A. Mol. Biomol. Spectrosc.* **60,** 527–534
10. Kubo, Y., Ikeda, T., Yang, S.-Y., and Tsuboi, M. (2000) *Appl. Spectrosc.* **54,** 1114–1119
11. Li, B., Mao, D., Liu, Y., Li, L., and Kuang, T. (2005) *Photosynth. Res.* **83,** 297–305
12. Edwards, H. G. M., de Oliveira, L. F. C., Cockell, C. S., Ellis-Evans, J. C., and Wynn-Williams, D. D. (2004) *Int. J. Astrobiol.* **3,** 125–129
13. Largeau, C., Casadevall, E., Berkaloff, C., and Dhamelincourt, P. (1980) *Phytochemistry* **19,** 1043–1051
14. Heraud, P., Wood, B. R., Beardall, J., and McNaughton, D. (2006) *J. Chemometrics* **20,** 193–197
15. Heraud, P., Beardall, J., McNaughton, D., and Wood, B. R. (2007) *FEMS Microbiol. Lett.* **275,** 24–30
16. Maxwell, J. R., Douglas, A. G., Eglinton, G., and McCormick, A. (1968) *Phytochemistry* **7,** 2157–2171
17. Knights, B. A., Brown, A. C., Conway, E., and Middleditch, B. S. (1970) *Phytochemistry* **9,** 1317–1324
18. Banerjee, A., Sharma, R., Chisti, Y., and Banerjee, U. C. (2002) *Crit. Rev. Biotechnol.* **22,** 245–279
19. Metzger, P., David, M., and Casadevall, E. (1987) *Phytochemistry* **26,** 129–134
20. Wolf, F. R., Nonomura, A. M., and Bassham, J. A. (1985) *J. Phycol.* **21,** 388–396
21. Templier, J., Largeau, C., and Casadevall, E. (1984) *Phytochemistry* **23,** 1017–1028
22. Metzger, P., Casadevall, E., Pouet, M. J., and Pouet, Y. (1985) *Phytochemistry* **24,** 2995–3002
23. Metzger, P., Templier, J., Largeau, C., and Casadevall, E. (1986) *Phytochemistry* **25,** 1869–1872
24. Templier, J., Largeau, C., and Casadevall, E. (1991) *Phytochemistry* **30,** 2209–2215
25. Metzger, P., and Casadevall, E. (1987) *Tetrahedron Lett.* **28,** 3911–3934
26. Metzger, P., Allard, B., Casadevall, E., Berkaloff, C., and Couté, A. (1990) *J. Phycol.* **26,** 258–266
27. Metzger, P., Casadevall, E., and Couté, A. (1988) *Phytochemistry* **27,** 1383–1388
28. Traverse, A. (1955) *Micropaleontology* **1,** 343–348
29. Cane, R. F. (1977) *Trans. R. Soc. S. Aust.* **101,** 153–154
30. Moldowan, J. M., and Seifert, W. K. (1980) *J. C. S. Chem. Commun.* **19,** 912–914
31. Brassell, S. C., Eglinton, G., and Mo, F. J. (1986) *Org. Geochem.* **10,** 927–941
32. McKirdy, D. M., Cox, R. E., Volkman, J. K., and Howell, V. J. (1986) *Nature* **320,** 57–59
33. Glikson, M., Lindsay, K., and Saxby, J. (1989) *Org. Geochem.* **14,** 595–608
34. Mastalerz, M., and Hower, J. C. (1996) *Org. Geochem.* **24,** 301–308
35. Stasiuk, L. D. (1999) *Org. Geochem.* **30,** 1021–1026
36. Testa, M., Gerbaudo, S., and Andri, E. (2001) *Proc. Ocean Drilling Program, Scientific Results* **180,** 1–6
37. Audino, M., Grice, K., Alexander, R., and Kagi, R. I. (2002) *Org. Geochem.* **33,** 979–984
38. Summons, R. E., Metzger, P., Largeau, C., Murray, A. P., and Hope, J. M. (2002) *Org. Geochem.* **33,** 99–109
39. Adam, P., Schaeffer, P., and Albrecht, P. (2006) *Org. Geochem.* **37,** 584–596
40. Okada, S., Devarenne, T. P., Murakami, M., Abe, H., and Chappell, J. (2004) *Arch. Biochem. Biophys.* **422,** 110–118
41. Sato, Y., Ito, Y., Okada, S., Murakami, M., and Abe, H. (2003) *Tetrahedron Lett.* **44,** 7035–7037
42. Huang, Z., and Poulter, C. D. (1989) *J. Am. Chem. Soc.* **111,** 2713–2715
43. Casadevall, E., Metzger, P., and Puech, M. P. (1984) *Tetrahedron Lett.* **25,** 4123–4126
44. Wolf, F. R., Nemethy, E. K., Blanding, J. H., and Bassham, J. A. (1985) *Phytochemistry* **24,** 733–737
45. Galbraith, M. N., Hillen, L. W., and Wake, L. V. (1983) *Phytochemistry* **22,** 1441–1443
46. Eroglu, E., and Melis, A. (2010) *Bioresource Technol.* **101,** 2359–2366
47. Nonomura, A. M. (1988) *Jpn. J. Phycol.* **36,** 285–291
48. Grung, M., Metzger, P., and Liaaen-Jensen, S. (1989) *Biochem. Syst. Ecol.* **17,** 263–269
49. Okada, S., Murakami, M., and Yamaguchi, K. (1995) *J. Appl. Phycol.* **7,** 555–559
50. Okada, S., Murakami, M., and Yamaguchi, K. (1997) *Phytochem. Anal.* **8,** 198–203
51. Frisch, M. J., Trucks, G. W., Schlegel, H. B., Scuseria, G. E., Robb, M. A.,

Cheeseman, J. R., Montgomery, J., Vreven, T., Kudin, K. N., Burant, J. C., Millam, J. M., Iyengar, S. S., Tomasi, J., Barone, V., Mennucci, B., Cossi, M., Scalmani, G., Rega, N., Petersson, G. A., Nakatsuji, H., Hada, M., Ehara, M., Toyota, K., Fukuda, R., Hasegawa, J., Ishida, M., Nakajima, T., Honda, Y., Kitao, O., Nakai, H., Klene, M., Li, X., Knox, J. E., Hratchian, H. P., Cross, J. B., Bakken, V., Adamo, C., Jaramillo, J., Gomperts, R., Stratmann, R. E., Yazyev, O., Austin, A. J., Cammi, R., Pomelli, C., Ochterski, J. W., Ayala, P. Y., Morokuma, K., Voth, G. A., Salvador, P., Dannenberg, J. J., Zakrzewski, V. G., Dapprich, S., Daniels, A. D., Strain, M. C., Farkas, O., Malick, D. K., Rabuck, A. D., Raghavachari, K., Foresman, J. B., Ortiz, J. V., Cui, Q., Baboul, A. G., Clifford, S., Cioslowski, J., Stefanov, B. B., Liu, G., Liashenko, A., Piskorz, P., Komaromi, I., Martin, R. L., Fox, D. J., Keith, T., Al-Laham, M. A., Peng, C. Y., Nanayakkara, A., Chalacombe, M., Gill, P. M. W., Johnson, B., Chen, W., Wong, M. W., Gonzalez, C., and Pople, J. A. (2004) GAUSSIAN, Version 0.3, Gaussian, Inc., Wallingford CT

52. Elsey, D., Jameson, D., Raleigh, B., and Cooney, M. J. (2007) *J. Microbiol. Methods* **68,** 639–642

53. Lee, S. J., Yoon, B.-D., and Oh, H.-M. (1998) *Biotech. Tech.* **12,** 553–556

54. Cooksey, K. E., Guckert, J. B., Williams, S. A., and Callis, P. R. (1987) *J. Microbial. Methods* **6,** 333–345

55. Huang, Z., and Poulter, C. D. (1989) *Phytochemistry* **28,** 3034–3046

56. Huang, Z., and Poulter, C. D. (1989) *Phytochemistry* **28,** 1467–1470

57. Achitouv, E., Metzger, P., Rager, M-N., and Largeau, C. (2004) *Phytochemistry* **65,** 3159–3165

58. Metzger, P., Rager, M. N., and Largeau, C. (2007) *Org. Geochem.* **38,** 566–581

59. Okada, S., Matsuda, H., Murakami, M., and Yamaguchi, K. (1996) *Tetrahedron Lett.* **37,** 1065–1068

60. Okada, S., Tonegawa, I., Matsuda, H., Murakami, M., and Yamaguchi, K. (1998) *Phytochemistry* **47,** 1111–1115